

Unsteady flow of a non-Newtonian second grade fluid in a channel partially filled by a porous medium

Dileep S. Chauhan* and Vikas Kumar

Department of Mathematics, University of Rajasthan, Jaipur, Rajasthan, India

ABSTRACT

A non-Newtonian second grade fluid flow is considered in a parallel plate horizontal channel partially filled by a porous medium. A porous layer of finite thickness is perfectly attached to upper stationary impermeable plate and the lower impermeable plate moves suddenly with a constant speed or it starts oscillating in its own plane with constant amplitude and frequency. The porous layer is assumed to be homogeneous with constant permeability and porosity. For flow in porous medium, a modified Darcy resistance term for a second grade fluid is taken in the momentum equation. Laplace transform method is applied to determine the solution of the unsteady flow problem for both cases. Expressions for velocity distributions in both porous and clear fluid regions, shear stresses at lower plate and porous interface are obtained, and the effects of the various pertinent parameters are investigated and discussed.

Key words: Unsteady flow; permeability; second grade fluid; channel partially filled with a porous medium.

INTRODUCTION

The study of fluid flow in the presence of porous media has become of main interest in many engineering and industrial applications, particularly when the flow is induced by shearing motion of a wall or convection and therefore such problems have been investigated extensively, e.g. Al-Nimr and Khadrawi [1], Bég et al. [2], Chauhan and Rastogi [3], Chauhan and Agrawal [4, 5], Saxena and Dubey [6], Sreekanth et al. [7], Sreenadh et al. [8] and Babu et al. [9]. It is interesting to investigate unsteady Couette flow in a parallel-plate channel filled or partially filled by a porous medium. The flow in the channel is caused by moving suddenly or oscillating one wall, while the other is kept at rest. Bhargava and Sacheti [10] examined generalized Couette flow of two immiscible fluids and heat transfer through a porous channel using Brinkman equations to govern the flow in porous medium.

The Couette flow of a high Prandtl number fluid of temperature dependent viscosity through a porous medium is investigated by Daskalakis [11]. Non-Darcy Couette flow through a porous medium saturated with an inelastic non-Newtonian fluid was examined by Nakayama [12]. Heat transfer effects in Couette flow were investigated by Chauhan and Shekhawat [13] and Chauhan and Soni [14] in the presence of a porous medium. Analytical study of Couette flow is conducted by Kuznetsov [15] in a parallel-plate channel partially filled by a porous medium and partially by a clear fluid. Chauhan and Gupta [16] studied heat transfer effects in Couette flow of a compressible fluid through a channel partially filled by a porous layer. Kuznetsov [17] investigated Couette flow and heat transfer in a composite duct.

Three dimensional Couette flow was investigated by Singh [18], Govindarajan [19] with transpiration cooling. The effects of permeability of a porous substrate are investigated by Chauhan and Kumar [20] in three-dimensional Couette flow in a composite parallel plate channel where a transverse sinusoidal injection velocity is applied at one bounding wall.

Apart from the direct engineering applications, the study of unsteady Couette flow is important because it can serve as a good estimate for initial velocities of more complex fluid flow situations. Jordan and Puri [21] obtained exact solutions of unsteady Couette dipolar fluid flow. Khaled and Vafai [22] determined exact solutions of Stokes and unsteady Couette flows for both small and large times under slip conditions. Unsteady MHD Couette flow and heat transfer was investigated by Attia [23, 24]. Such MHD flow and heat transfer problem in a porous medium is investigated by Bég *et al.* [25]. Umavathi *et al.* [26] studied unsteady oscillating fluid flow in a composite porous medium parallel-plate channel.

Recently the study of non-Newtonian fluid flows in the presence of a porous medium has gained interest considerably due to their several engineering applications in ceramic processing, biomechanics, enhanced oil recovery process and filtration process. However the governing equations that describe such fluid flows are complex and the exact solutions for these problems are rare. For one subclass of differential-type non-Newtonian fluids (second grade fluid), researchers obtain exact solutions for particular flow problems. Tan *et al.* [27] determined an exact solution of unsteady plane Couette flow of second grade fluid. Using fractional derivative model Tan and Xu [28] studied unsteady flows of a second grade fluid between two parallel plates in various cases. Erdoğan and Imrak [29] investigated effects of side walls on the unsteady flow of a second grade fluid in a duct. Jordan and Puri [30], and Tan and Masuoka [31] examined Stokes first problem for a second grade fluid in a porous half-space. Hayat *et al.* [32] discussed the flow of a second grade fluid in a parallel-plate channel filled by a porous medium when one of the plates is moved suddenly and other is kept at rest. And in the other case, unsteady flow problem is examined when one plate is oscillating and the other is at rest. Analytic solutions of these problems are determined using Laplace transform method.

In this paper, a second grade fluid between two horizontal parallel plates is considered, where a porous layer of finite thickness is perfectly attached to the upper plate. Both plates and fluid are initially at rest, and the unsteady flow in the channel is generated by sudden motion of the lower impermeable plate or oscillation of the lower plate with a constant frequency in its own plane. Exact solutions are obtained for these two cases, and the effects of the various pertinent parameters are shown graphically and discussed.

MATERIALS AND METHODS

Formulation and solution

We consider the flow of a second grade non-Newtonian fluid between two horizontal parallel impermeable plates. The distance between two plates is h and a porous layer of thickness $h-d$ is attached to the upper plate, in the channel. A Cartesian coordinate system is taken. x -axis is taken along the lower plate, and y -axis is normal to the channel. Thus lower plate is at $y=0$, porous medium interface in the channel is at $y=d$, and upper plate is at $y=h$. The second grade fluid fills the channel $0 \leq y \leq d$ and the porous layer $d \leq y \leq h$. We write these two regions as clear fluid region-I and porous medium region-II respectively. Both plates and fluid are initially at rest. Unsteady flow is generated in the channel due to sudden motion of the lower plate with constant speed U_0 or oscillation of the lower plate with frequency ω in its own plane. We investigate the unsteady motion in the channel partially filled with a porous medium for these two cases as (i) First problem, and (ii) Second problem.

For a second grade fluid, Cauchy stress tensor \bar{T} is given by the constitutive equation,

$$\bar{T} = -p\bar{I} + \mu\bar{A}_1 + \alpha_1\bar{A}_2 + \alpha_2\bar{A}_1^2, \quad (1)$$

where p is the pressure, \bar{I} is the unit tensor, μ is the dynamic viscosity, α_1 and α_2 are the normal stress moduli and \bar{A}_1 and \bar{A}_2 are first two Rivlin-Ericksen kinematic tensors (Fosdick and Rajagopal [33]) defined by

$$\bar{A}_1 = \nabla\bar{V} + (\nabla\bar{V})^*, \quad (2)$$

$$\bar{A}_2 = \frac{d\bar{A}_1}{dt} + \bar{A}_1(\nabla\bar{V}) + (\nabla\bar{V})^*\bar{A}_1, \quad (3)$$

where d/dt denotes the material time derivative, \bar{V} is the velocity field and grad is the gradient operator, and $(*)$ is the matrix transpose.

If the second-grade fluid given by (1) is compatible with thermodynamics, then the material moduli must meet the following restriction (Dunn and Rajagopal [34])

$$\mu \geq 0, \alpha_1 \geq 0 \text{ and } \alpha_1 + \alpha_2 = 0. \quad (4)$$

For the unsteady flow in porous medium, the Darcy resistance for a second-grade fluid, which is a measure of the flow resistance offered by the solid matrix, following Vafai and Tien [35], is given by

$$\bar{\mathbf{r}} = -\frac{\varepsilon}{K} \left(\mu + \alpha_1 \frac{\partial}{\partial t} \right) \bar{\mathbf{v}}, \quad (5)$$

where, K , the permeability and ε is the porosity of the porous medium.

By introducing the following dimensionless quantities,

$$u^* = u/U_0, y^* = y/h, t^* = vt/h^2, \omega^* = h^2\omega/\nu, \sigma = h\sqrt{\varepsilon/K}, \alpha = \alpha_1/\rho h^2, a = d/h, \quad (6)$$

the governing dimensionless equations for both regions become

For clear fluid region ($0 \leq y \leq a$) – I

$$\frac{\partial u}{\partial t} = \frac{\partial^2 u}{\partial y^2} + \alpha \frac{\partial^3 u}{\partial y^2 \partial t}, \quad (7)$$

For porous medium region ($a \leq y \leq 1$) – II

$$(1 + \sigma^2 \alpha) \frac{\partial U}{\partial t} = \frac{\partial^2 U}{\partial y^2} + \alpha \frac{\partial^3 U}{\partial y^2 \partial t} - \sigma^2 U, \quad (8)$$

where, ρ , the fluid density; σ , the permeability parameter and α is the non-Newtonian parameter.

The corresponding dimensionless boundary and initial condition for these two problems are given by

For first problem

$$\begin{aligned} \text{at } y=0; & \quad u(0,t)=1, \\ \text{at } y=a; & \quad u(a,t)=U(a,t), \quad \left. \frac{\partial u(y,t)}{\partial y} \right|_{y=a} = \left. \frac{\partial U(y,t)}{\partial y} \right|_{y=a}, \\ \text{at } y=1; & \quad U(1,t)=0, \\ \text{and} & \quad u(y,0)=0, U(y,0)=0. \end{aligned} \quad (9)$$

For second problem

$$\begin{aligned} \text{at } y=0; & \quad u(0,t)=\exp(i\omega t), \\ \text{at } y=a; & \quad u(a,t)=U(a,t), \quad \left. \frac{\partial u(y,t)}{\partial y} \right|_{y=a} = \left. \frac{\partial U(y,t)}{\partial y} \right|_{y=a}, \\ \text{at } y=1; & \quad U(1,t)=0, \\ \text{and} & \quad u(y,0)=0, U(y,0)=0. \end{aligned} \quad (10)$$

Exact solutions are obtained of these two problems using Laplace transform method, by defining

$$\bar{u}(y, s) = L[u(y, t)] = \int_0^{\infty} \exp(-st) u(y, t) dt, \quad (11)$$

and

$$\bar{U}(y, s) = L[U(y, t)] = \int_0^{\infty} \exp(-st) U(y, t) dt. \quad (12)$$

Here s is a Laplace transform parameter.

Using above, equations (7) and (8) reduces to

$$\bar{u}'' - (s/(1 + \alpha s)) \bar{u} = 0, \quad (13)$$

$$\bar{U}'' - \left(\frac{\sigma^2 + s(1 + \sigma^2 \alpha)}{1 + \alpha s} \right) \bar{U} = 0, \quad (14)$$

with the corresponding boundary conditions

For first problem

$$\begin{aligned} \text{at } y=0; & \quad \bar{u}(0, s) = 1/s, \\ \text{at } y=a; & \quad \bar{u}(a, s) = \bar{U}(a, s), \quad \left. \frac{\partial \bar{u}(y, s)}{\partial y} \right|_{y=a} = \left. \frac{\partial \bar{U}(y, s)}{\partial y} \right|_{y=a}, \\ \text{at } y=1; & \quad \bar{U}(1, s) = 0, \end{aligned} \quad (15)$$

For second problem

$$\begin{aligned} \text{at } y=0; & \quad \bar{u}(0, s) = 1/(s - i\omega), \\ \text{at } y=a; & \quad \bar{u}(a, s) = \bar{U}(a, s), \quad \left. \frac{\partial \bar{u}(y, s)}{\partial y} \right|_{y=a} = \left. \frac{\partial \bar{U}(y, s)}{\partial y} \right|_{y=a}, \\ \text{at } y=1; & \quad \bar{U}(1, s) = 0, \end{aligned} \quad (16)$$

The solutions of equation (13) and (14) under the boundary conditions (15) are given by

$$\bar{u} = A \sinh py + B \cosh py, \quad (17)$$

$$\bar{U} = C \sinh qy + D \cosh qy. \quad (18)$$

Where,

$$p = \left[\frac{s}{1 + \alpha s} \right]^{1/2}, \quad q = \left[\frac{\sigma^2 + s(1 + \sigma^2 \alpha)}{1 + \alpha s} \right]^{1/2},$$

$$A = \frac{p \sinh ap \sinh(a-1)q - q \cosh ap \cosh(a-1)q}{s [q \sinh ap \cosh(a-1)q - p \cosh ap \sinh(a-1)q]}, \quad B = \frac{1}{s},$$

$$C = \frac{-p \cosh q}{s [q \sinh ap \cosh(a-1)q - p \cosh ap \sinh(a-1)q]}, \quad D = -C \tanh q.$$

Above equations has a simple pole at $s = 0$. It has an infinite number of poles located on the negative real axis at $s_n = -j_n^2 / (1 + \alpha j_n^2)$, where j_n is a real number and n changes from one to infinity. These j_n can be determined

by the following equation

$$\sqrt{j_n^2 - \sigma^2} \tan(\alpha j_n) + j_n \tan(1 - \alpha) \sqrt{j_n^2 - \sigma^2} = 0. \quad (19)$$

Also the solutions of equation (13) and (14) under the boundary conditions (16) are given by

$$\bar{u} = A' \sinh py + B' \cosh py, \quad (20)$$

$$\bar{U} = C' \sinh qy + D' \cosh qy. \quad (21)$$

Where,

$$A' = \frac{p \sinh ap \sinh(a-1)q - q \cosh ap \cosh(a-1)q}{(s - i\omega) [q \sinh ap \cosh(a-1)q - p \cosh ap \sinh(a-1)q]}, \quad B' = \frac{1}{s - i\omega},$$

$$C' = \frac{-p \cosh q}{(s - i\omega) [q \sinh ap \cosh(a-1)q - p \cosh ap \sinh(a-1)q]}, \quad D' = -C' \tanh q.$$

Above equations has a simple pole at $s = i\omega$. It has an infinite number of poles located on the negative real axis at $s_n = -j_n^2 / (1 + \alpha j_n^2)$, where j_n is a real number and n changes from one to infinity. These j_n can also be determined by the equation (19).

Using the Cauchy's residue theorem (Brown and Churchill, [36]) and complex analysis, the inverse Laplace transform of the velocity is obtained.

(A) Solutions for the first problem are given by

$$u(y, t) = 1 - \frac{\sigma y \cosh(1-a)\sigma}{a\sigma \cosh(1-a)\sigma + \sinh(1-a)\sigma} + 2 \sum_{n=1}^{\infty} \frac{\sqrt{j_n^2 - \sigma^2} F_1(j_n) \sin(j_n y)}{j_n (1 + \alpha j_n^2) F_2(j_n)} \exp\left(-\frac{j_n^2}{1 + \alpha j_n^2} t\right), \quad (22)$$

$$U(y, t) = \frac{\sinh(1-y)\sigma}{a\sigma \cosh(1-a)\sigma + \sinh(1-a)\sigma} + 2 \sum_{n=1}^{\infty} \frac{\sqrt{j_n^2 - \sigma^2} \sin\left\{(1-y)\sqrt{j_n^2 - \sigma^2}\right\}}{(1 + \alpha j_n^2) F_2(j_n)} \exp\left(-\frac{j_n^2}{1 + \alpha j_n^2} t\right). \quad (23)$$

The steady state solution is of the following form:

$$u(y, t) = 1 - \frac{\sigma y \cosh(1-a)\sigma}{a\sigma \cosh(1-a)\sigma + \sinh(1-a)\sigma}, \quad (24)$$

$$U(y, t) = \frac{\sinh(1-y)\sigma}{a\sigma \cosh(1-a)\sigma + \sinh(1-a)\sigma}. \quad (25)$$

The volume flux Q across a plane normal to the flow is

$$Q = \int_0^a u dy + \int_a^1 U dy. \quad (26)$$

Using (22) and (23), we get from equation (26)

$$Q = a - \frac{\sigma a^2 \cosh(1-a)\sigma}{2[\sinh(1-a)\sigma + a\sigma \cosh(1-a)\sigma]} - \frac{1 - \cosh(1-a)\sigma}{\sigma[\sinh(1-a)\sigma + a\sigma \cosh(1-a)\sigma]} + 2 \sum_{n=1}^{\infty} \frac{\sqrt{j_n^2 - \sigma^2} F_1(j_n)(1 - \cos j_n a)}{j_n^2 (1 + \alpha j_n^2) F_2(j_n)} \exp\left(-\frac{j_n^2}{1 + \alpha j_n^2} t\right) + 2 \sum_{n=1}^{\infty} \frac{[1 - \cos\{(1-a)\sqrt{j_n^2 - \sigma^2}\}]}{(1 + \alpha j_n^2) F_2(j_n)} \exp\left(-\frac{j_n^2}{1 + \alpha j_n^2} t\right). \quad (27)$$

The dimensionless shear stress at the lower moving wall ($y = 0$),

$$\tau_0 = \left(\frac{\partial u}{\partial y} + \alpha \frac{\partial^2 u}{\partial y \partial t} \right)_{y=0} = -\frac{\sigma \cosh(1-a)\sigma}{a\sigma \cosh(1-a)\sigma + \sinh(1-a)\sigma} + 2 \sum_{n=1}^{\infty} \frac{\sqrt{j_n^2 - \sigma^2} F_1(j_n)}{(1 + \alpha j_n^2)^2 F_2(j_n)} \exp\left(-\frac{j_n^2}{1 + \alpha j_n^2} t\right), \quad (28)$$

and at the porous medium interface ($y = a$),

$$\tau_a = \left(\frac{\partial u}{\partial y} + \alpha \frac{\partial^2 u}{\partial y \partial t} \right)_{y=a} = -\frac{\sigma \cosh(1-a)\sigma}{a\sigma \cosh(1-a)\sigma + \sinh(1-a)\sigma} + 2 \sum_{n=1}^{\infty} \frac{\sqrt{j_n^2 - \sigma^2} F_1(j_n) \cos(j_n a)}{(1 + \alpha j_n^2)^2 F_2(j_n)} \exp\left(-\frac{j_n^2}{1 + \alpha j_n^2} t\right). \quad (29)$$

(B) Solutions for the second problem are given by

$$u(y, t) = \frac{[m \cosh(1-a)m \sinh(a-y)l + l \sinh(1-a)m \cosh(a-y)l] \exp(i\omega t)}{m \sinh al \cosh(1-a)m + l \cosh al \sinh(1-a)m} + 2 \sum_{n=1}^{\infty} \frac{j_n \sqrt{j_n^2 - \sigma^2} F_1(j_n) \sin(j_n y)}{F_2(j_n) F_3(j_n)} \exp\left(-\frac{j_n^2}{1 + \alpha j_n^2} t\right), \quad (30)$$

$$U(y, t) = \frac{[l \sinh(1-y)m] \exp(i\omega t)}{m \sinh al \cosh(1-a)m + l \cosh al \sinh(1-a)m} + 2 \sum_{n=1}^{\infty} \frac{j_n^2 \sqrt{j_n^2 - \sigma^2} \sin\{(1-y)\sqrt{j_n^2 - \sigma^2}\}}{F_2(j_n) F_3(j_n)} \exp\left(-\frac{j_n^2}{1 + \alpha j_n^2} t\right). \quad (31)$$

The steady state solution is of the following form

$$u(y, t) = \frac{[m \cosh(1-a)m \sinh(a-y)l + l \sinh(1-a)m \cosh(a-y)l] \exp(i\omega t)}{m \sinh al \cosh(1-a)m + l \cosh al \sinh(1-a)m}, \quad (32)$$

$$U(y,t) = \frac{[l \sinh(1-y)m] \exp(i\omega t)}{m \sinh al \cosh(1-a)m + l \cosh al \sinh(1-a)m} \quad (33)$$

The volume flux Q across a plane normal to the flow is

$$Q = \int_0^a u dy + \int_a^1 U dy \quad (34)$$

Using (30) and (31), we get from equation (34)

$$Q = \frac{[m^2 \cosh(1-a)m \cosh al + lm \sinh(1-a)m \sinh al + (l^2 - m^2) \cosh(1-a)m - l^2] \exp(i\omega t)}{lm [m \sinh al \cosh(1-a)m + l \cosh al \sinh(1-a)m]} \\ + 2 \sum_{n=1}^{\infty} \frac{\sqrt{j_n^2 - \sigma^2} F_1(j_n) (1 - \cos j_n a)}{F_2(j_n) F_3(j_n)} \exp\left(-\frac{j_n^2 t}{1 + \alpha j_n^2}\right) \\ + 2 \sum_{n=1}^{\infty} \frac{j_n^2 [1 - \cos\{(1-a)\sqrt{j_n^2 - \sigma^2}\}]}{F_2(j_n) F_3(j_n)} \exp\left(-\frac{j_n^2 t}{1 + \alpha j_n^2}\right) \quad (35)$$

The dimensionless shear stress at the oscillating plate ($y = 0$),

$$\tau_0 = \left(\frac{\partial u}{\partial y} + \alpha \frac{\partial^2 u}{\partial y \partial t} \right)_{y=0} \\ = - \frac{l(1+i\alpha\omega) [m \cosh(1-a)m \cosh al + l \sinh(1-a)m \sinh al] \exp(i\omega t)}{m \sinh al \cosh(1-a)m + l \cosh al \sinh(1-a)m} \\ + 2 \sum_{n=1}^{\infty} \frac{j_n^2 \sqrt{j_n^2 - \sigma^2} F_1(j_n)}{(1 + \alpha j_n^2) F_2(j_n) F_3(j_n)} \exp\left(-\frac{j_n^2 t}{1 + \alpha j_n^2}\right) \quad (36)$$

and at the porous medium interface ($y = a$),

$$\tau_a = - \left(\frac{\partial U}{\partial y} + \alpha \frac{\partial^2 U}{\partial y \partial t} \right)_{y=a} \\ = \frac{lm(1+i\alpha\omega) \cosh(1-a)m \exp(i\omega t)}{m \sinh al \cosh(1-a)m + l \cosh al \sinh(1-a)m} \\ + 2 \sum_{n=1}^{\infty} \frac{j_n^2 (j_n^2 - \sigma^2) \cos(1-a) \sqrt{j_n^2 - \sigma^2}}{(1 + \alpha j_n^2) F_2(j_n) F_3(j_n)} \exp\left(-\frac{j_n^2 t}{1 + \alpha j_n^2}\right) \quad (37)$$

Where

$$l = \left(\frac{\alpha \omega^2 + i\omega}{1 + \alpha^2 \omega^2} \right)^{1/2}, \quad m = \left(\frac{\beta^2 (1 + \alpha^2 \omega^2) + \alpha \omega^2 + i\omega}{1 + \alpha^2 \omega^2} \right)^{1/2}$$

$$F_1(j_n) = \left[j_n \sin a j_n \sin\{(1-a)\sqrt{j_n^2 - \sigma^2}\} - \sqrt{j_n^2 - \sigma^2} \cos a j_n \cos\{(1-a)\sqrt{j_n^2 - \sigma^2}\} \right]$$

$$F_2(j_n) = \left[j_n \sin a j_n \cos\{(1-a)\sqrt{j_n^2 - \sigma^2}\} + (j_n^2 - a\sigma^2) \cos a j_n \cos\{(1-a)\sqrt{j_n^2 - \sigma^2}\} \right]$$

$$-j_n \sqrt{j_n^2 - \sigma^2} \sin a j_n \sin \left\{ (1-a) \sqrt{j_n^2 - \sigma^2} \right\} + \sqrt{j_n^2 - \sigma^2} \cos a j_n \sin \left\{ (1-a) \sqrt{j_n^2 - \sigma^2} \right\} \Big] \\ F_3(j_n) = (1 + \alpha j_n^2) \left[j_n^2 + i\omega(1 + \alpha j_n^2) \right]$$

RESULTS AND DISCUSSION

In this paper, the unsteady shearing motion of a second grade fluid between two horizontal parallel plates is investigated, where a porous layer of finite thickness is perfectly attached to the upper stationary plate and unsteady flow in the channel is generated either by sudden motion of the lower plate or by oscillating it in its own plane. Exact solutions are obtained for the first and second problem by the Laplace transform method, such that these represent unsteady flows in the channel at the time $t = 0^+$ and for $t \rightarrow \infty$ they become steady state solutions. The effects of various pertinent parameters on the flow and shear stresses at the boundary walls of the channel are shown in figs. 1-11. In each figure part (a) is drawn for the first problem, while part (b) and (c) describes the second problem. The effects of time can be observed by figs. 1-3 on the velocity distribution in the channel for both problems.

In fig. 1(a), we see that with the increase in time t , the flow approaches a steady state in the first problem. It is achieved at $t = 0.4$, when $\sigma = 10$ and $\alpha = 0.01$. If we compare fig. 1(a) with the case when $K \rightarrow \infty$ ($\sigma = 0$) (fig. 2(a)), i.e. the channel is free from the porous material, we see that by the introduction of the porous layer in the channel the steady state is achieved earlier. Figure 1(a) is also compared with the case when $\alpha = 0$ (fig. 3(a)), i.e. the channel is filled with Newtonian fluid. It can be seen that the flow of a Newtonian fluid gets to the steady state more quickly than that of a second grade fluid. Similar results are observed for the second problem, except that in this case the steady state is achieved much later when compared to the first problem. Results are also compared for the case when the channel is completely filled by a porous medium for both problems.

Equations (24) and (25) reveal that the steady state solution of the coupled flow first problem is independent of the non-Newtonian parameter. Therefore the steady state velocity profiles in both regions are same for the Newtonian and second grade fluid. However, the transient solution is affected by the nature of the fluid. On the other hand, eq. (32) and (33) show that in second problem, the periodic steady state solution and the transient solution both depends on the non-Newtonian parameter. It is apparent from the fig. 4 that velocity is an increasing function of the non-Newtonian parameter in both the problems. Also the effect of non-Newtonian parameter on transient velocity is shown in fig. 5. We see that the transient velocity decrease numerically on increasing the non-Newtonian parameter.

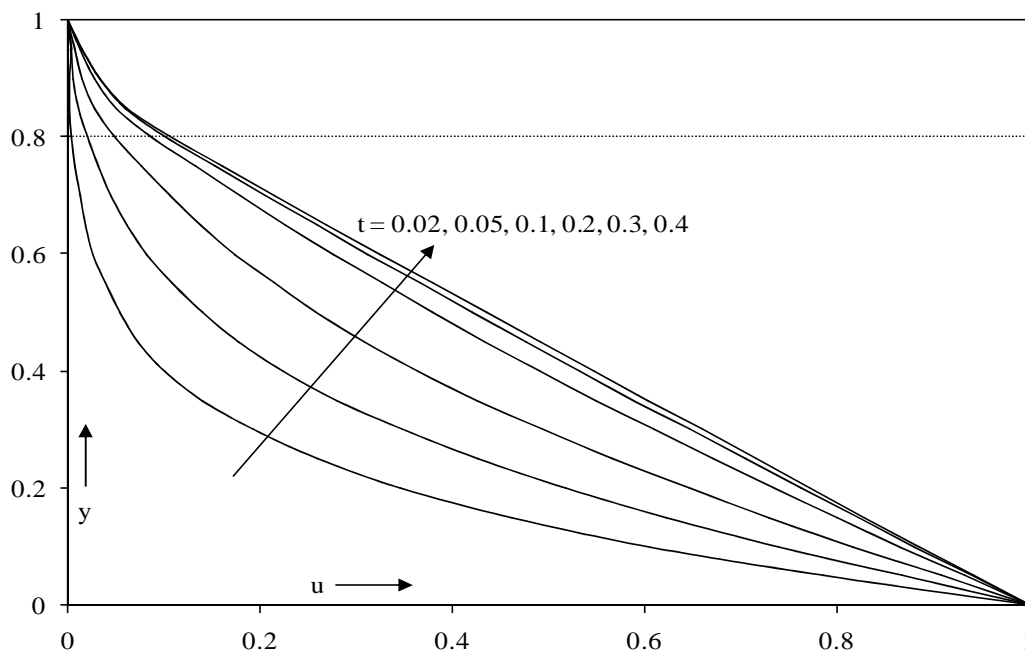


Fig. 1(a) Profiles of the dimensionless velocity $u(y)$ against y for $\sigma = 10$, $\alpha = 0.01$, $a = 0.8$ (the first problem)

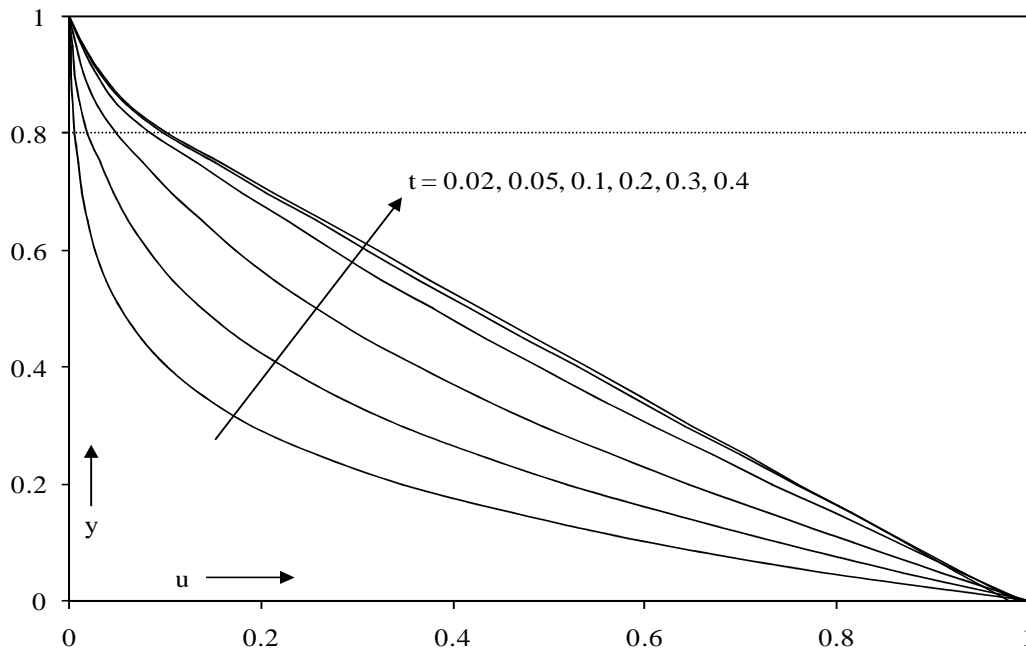


Fig. 1(b) Profiles of the dimensionless velocity $u(y)$ against y for $\sigma = 10, \alpha = 0.01, \omega = 0.5, a = 0.8$ (the second problem)

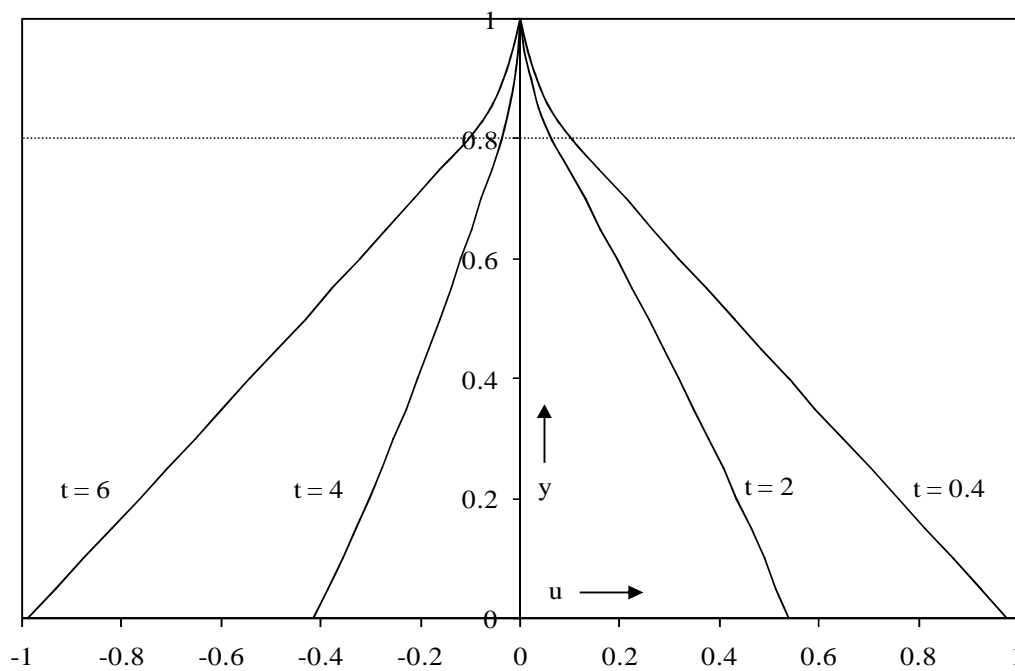


Fig. 1(c) Profiles of the dimensionless velocity $u(y)$ against y for $\sigma = 10, \alpha = 0.01, \omega = 0.5, a = 0.8$ (the second problem)

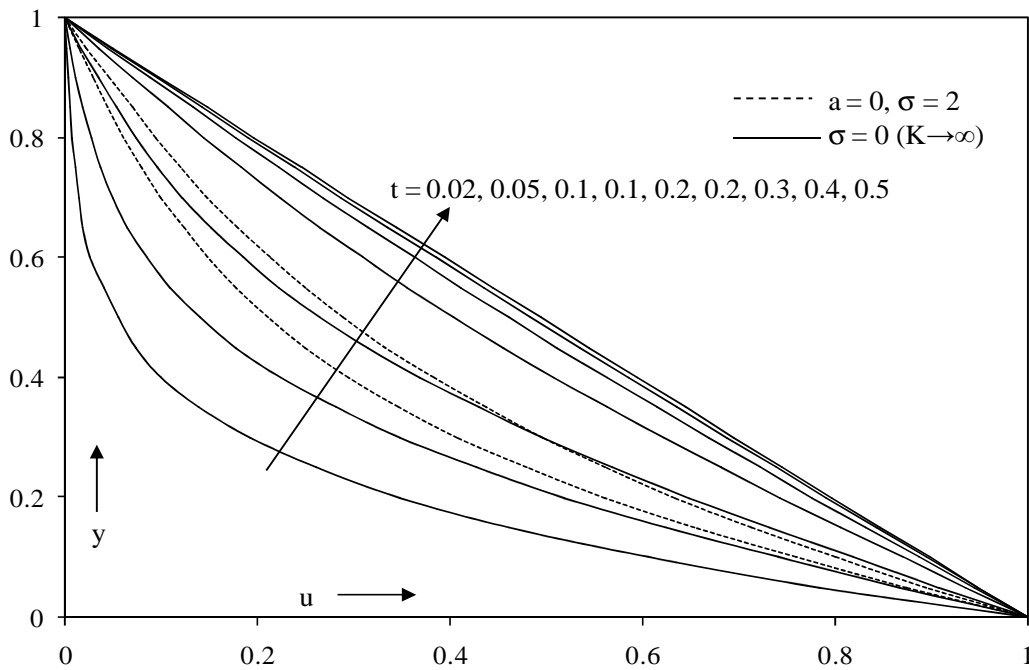


Fig. 2(a) Profiles of the dimensionless velocity $u(y)$ against y for $\alpha = 0.01$ (the first problem)

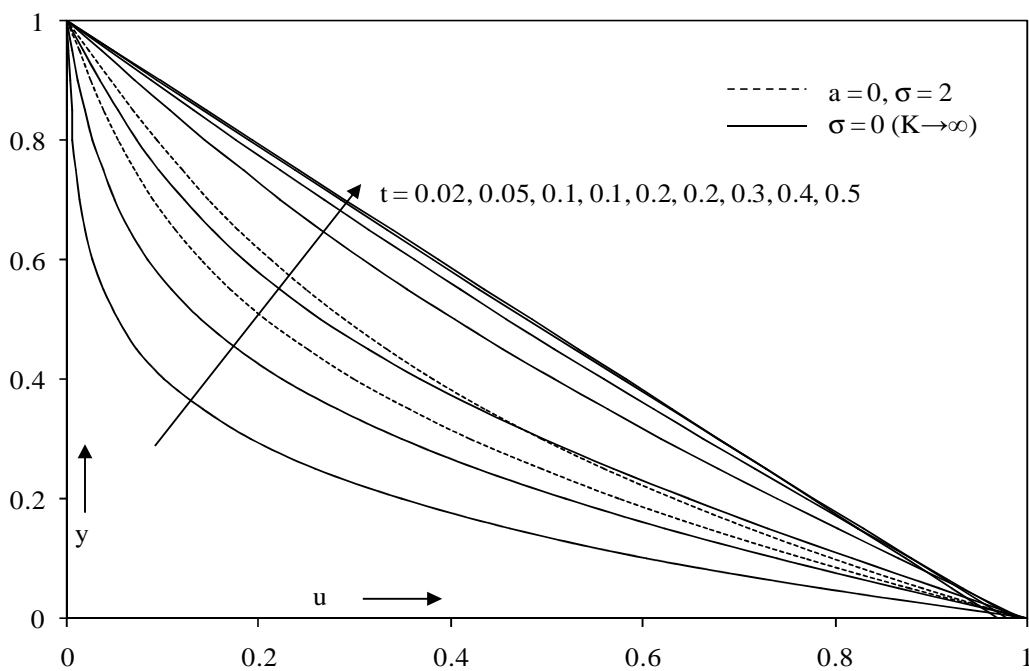


Fig. 2(b) Profiles of the dimensionless velocity $u(y)$ against y for $\alpha = 0.01, \omega = 0.5$ (the second problem)

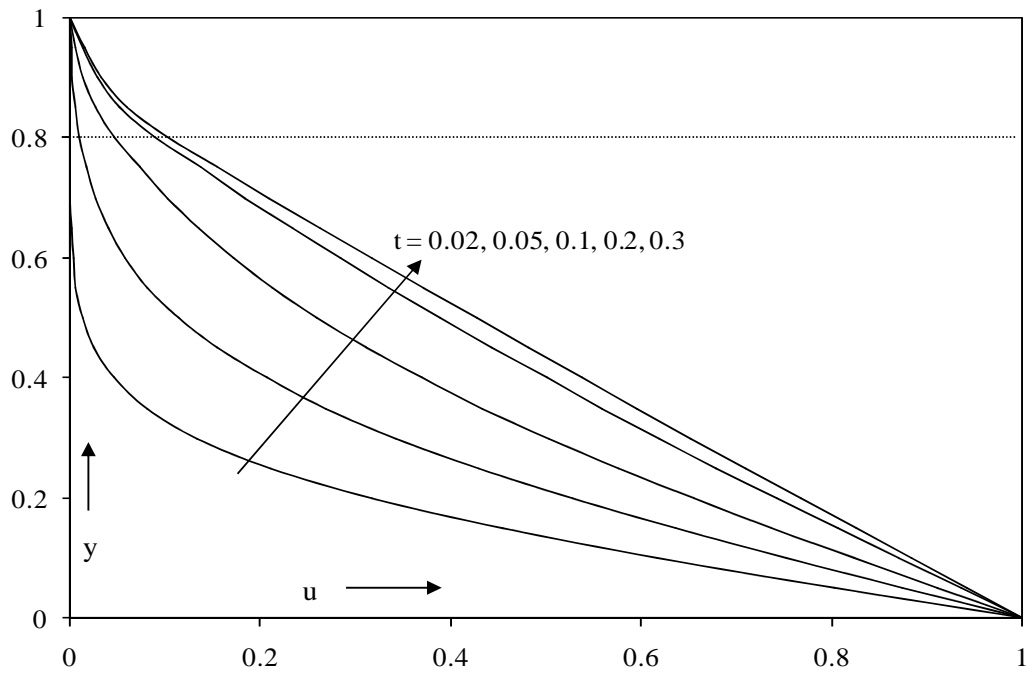


Fig. 3(a) Profiles of the dimensionless velocity $u(y)$ against y for $\sigma = 10, \alpha = 0, a = 0.8$ (the first problem)

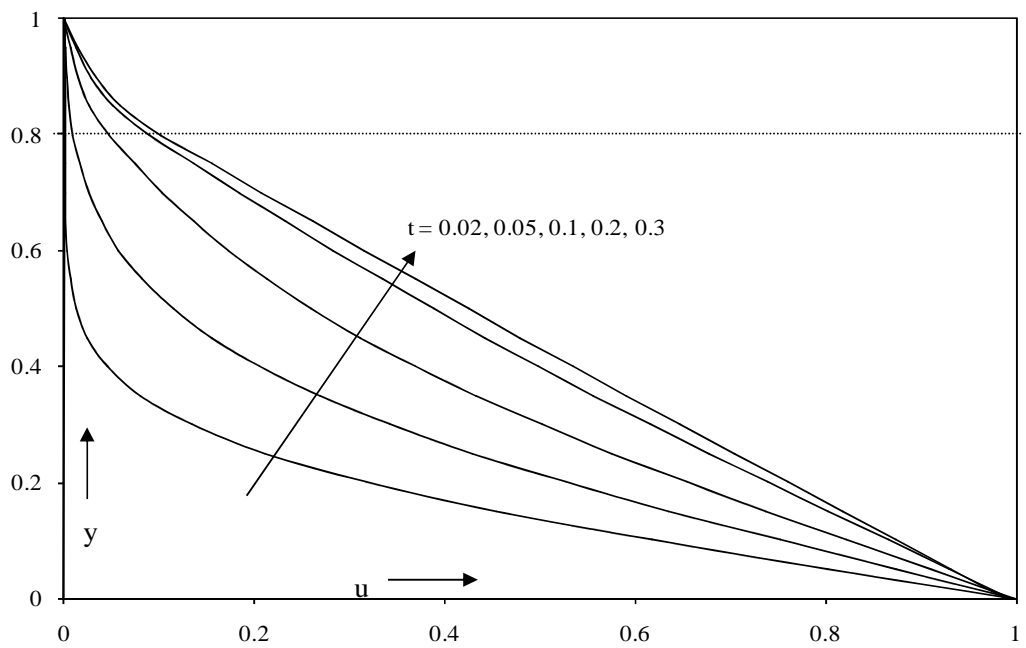


Fig. 3(b) Profiles of the dimensionless velocity $u(y)$ against y for $\sigma = 10, \alpha = 0, \omega = 0.5, a = 0.8$ (the second problem)

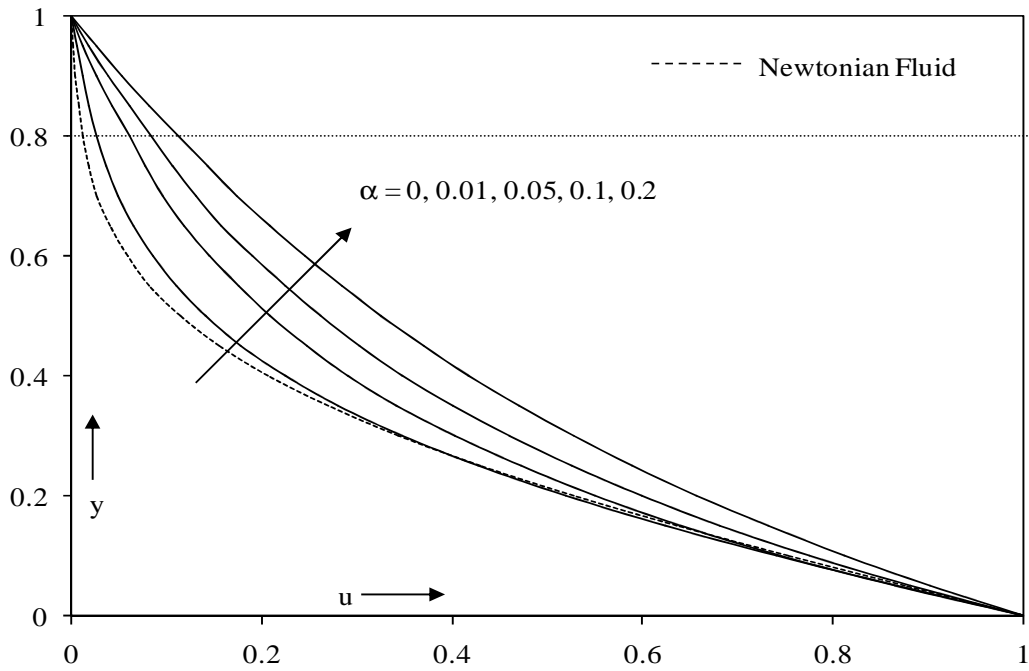


Fig. 4(a) Profiles of the dimensionless velocity $u(y)$ against y for $\sigma = 2, t = 0.05, a = 0.8$ (the first problem)

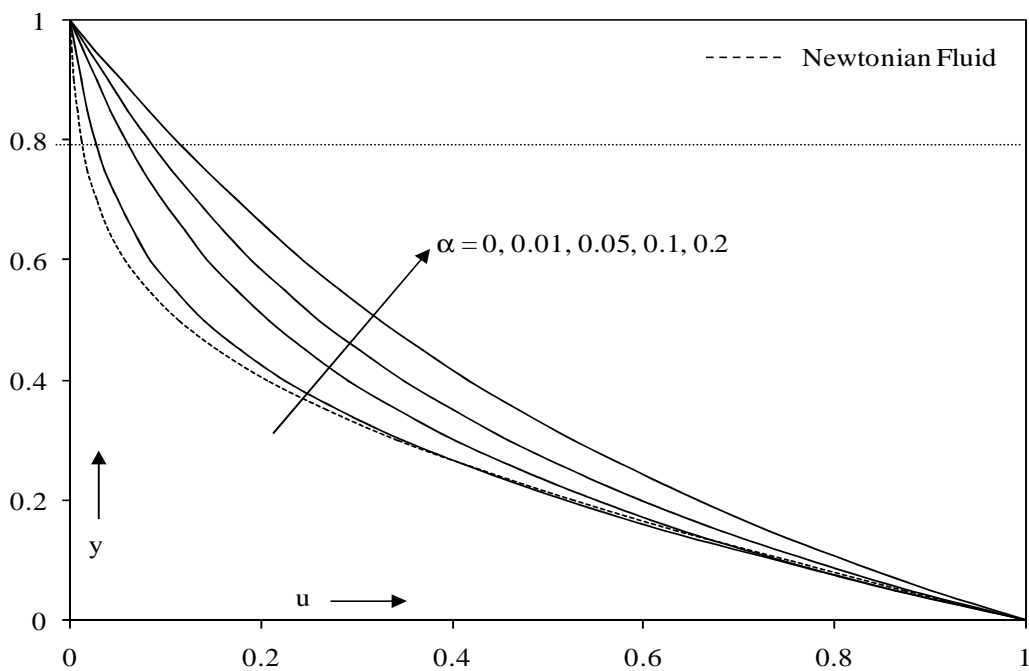


Fig. 4(b) Profiles of the dimensionless velocity $u(y)$ against y for $\sigma = 2, t = 0.05, \omega = 0.5, a = 0.8$ (the first problem)

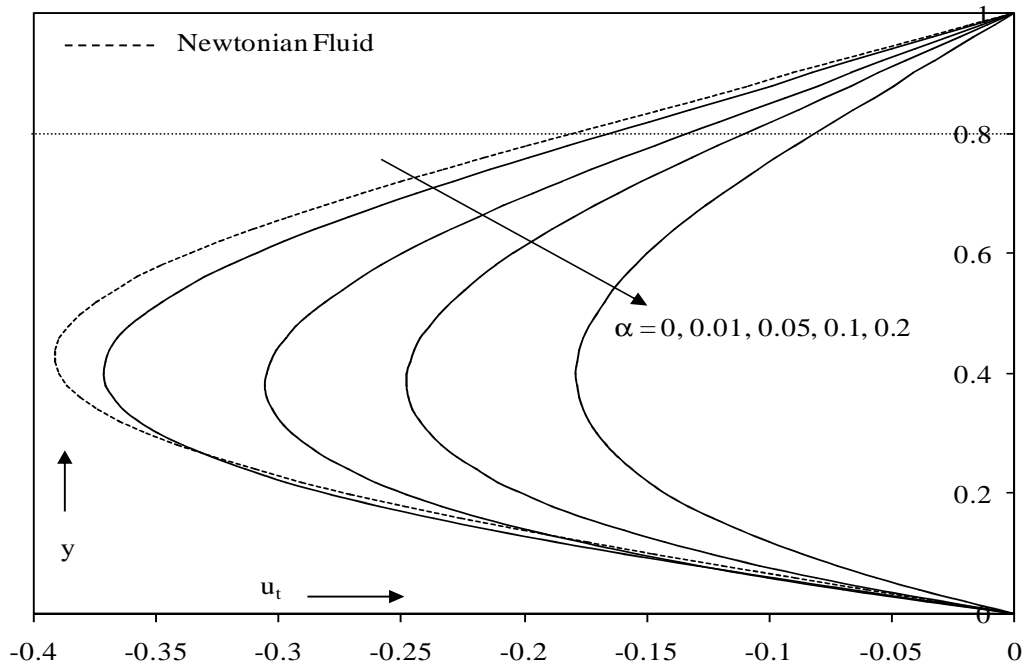


Fig. 5(a) Profiles of the dimensionless transient velocity $u_t(y)$ against y for $\sigma = 2, t = 0.05, a = 0.8$ (the first problem)

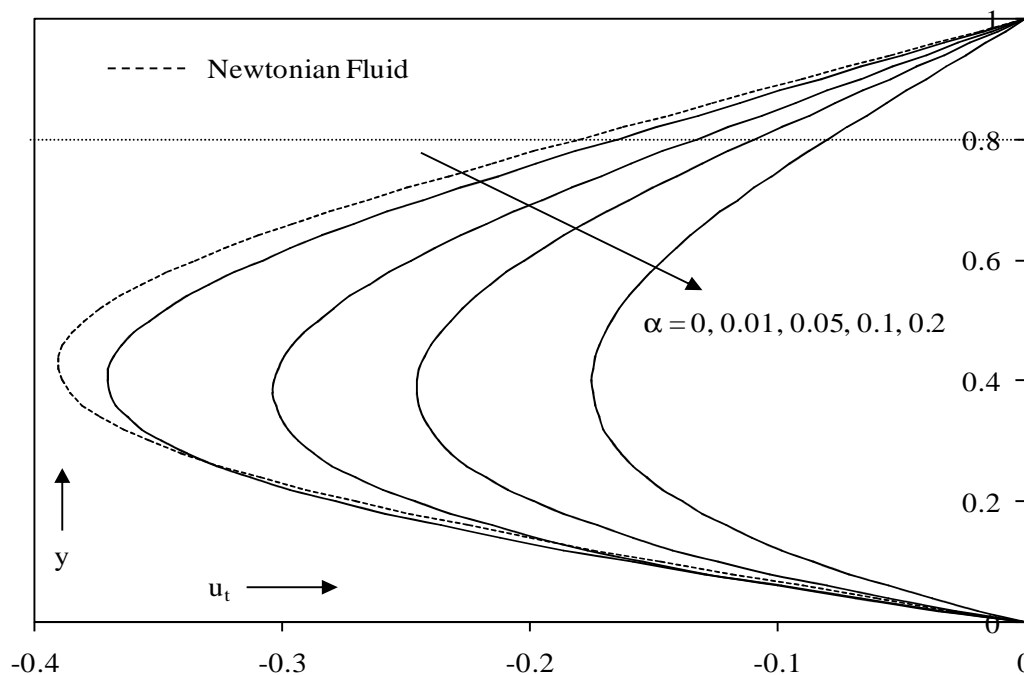


Fig. 5(b) Profiles of the dimensionless transient velocity $u_t(y)$ against y for $\sigma = 2, t = 0.05, \omega = 0.5, a = 0.8$ (the second problem)

In figs. 6-8, we see that the effect of the permeability K is to increase the flow in both clear fluid and porous region. The steady state velocity is an increasing function of K , and the transient flow velocity also increases numerically throughout the region with an increase in permeability for both the problems. It is seen that the effect of the permeability is significant only in the porous layer and in the nearby porous interface region in the clear fluid.

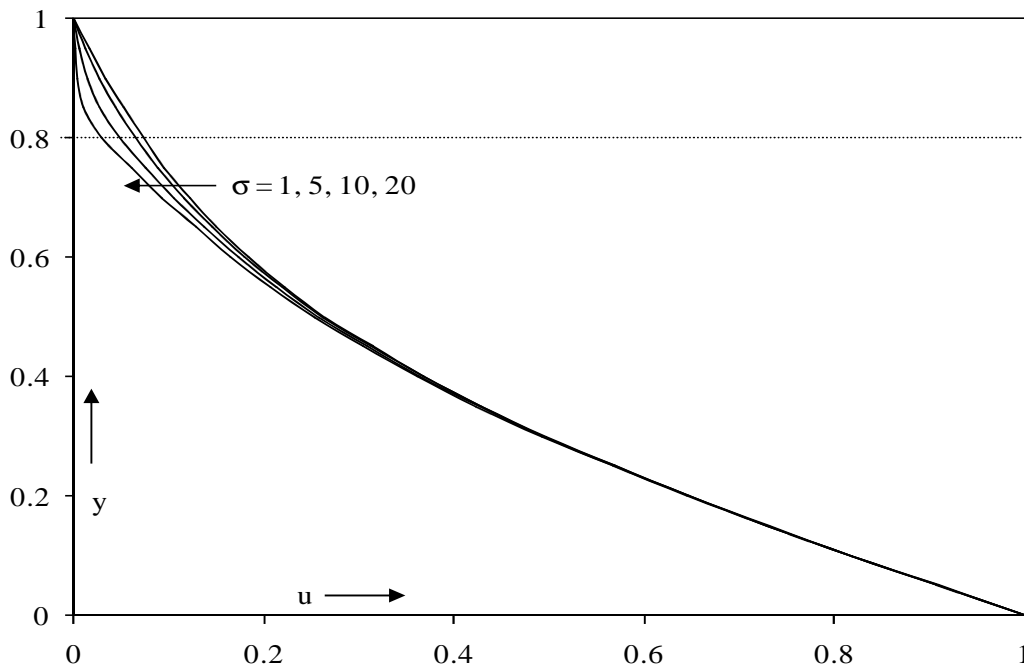


Fig. 6(a) Profiles of the dimensionless velocity $u(y)$ against y for $\alpha = 0.01, t = 0.1, a = 0.8$ (the first problem)

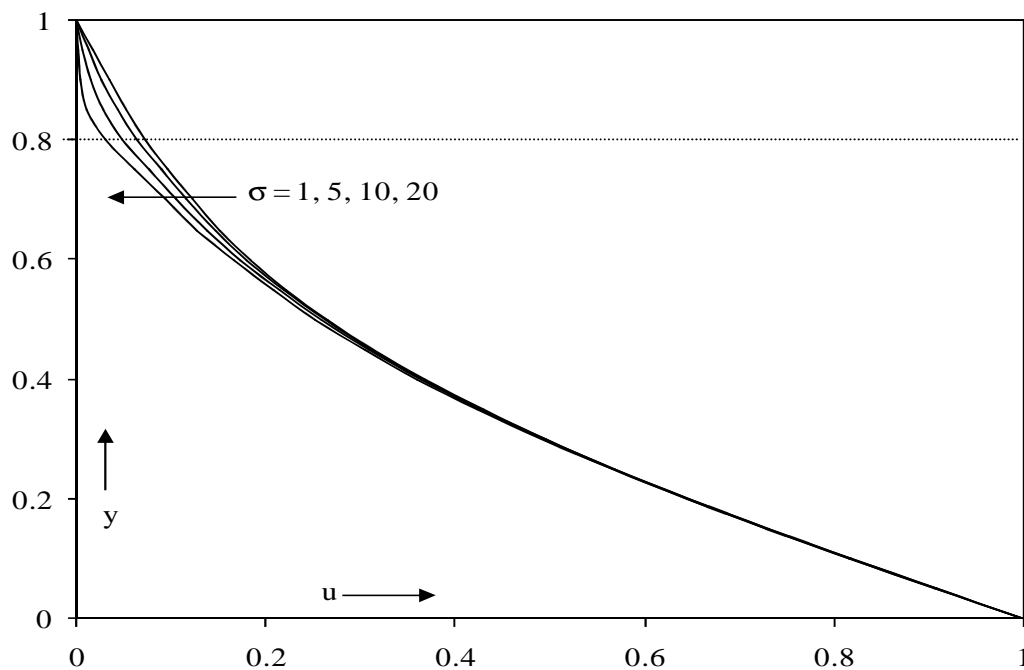


Fig. 6(b) Profiles of the dimensionless velocity $u(y)$ against y for $\alpha = 0.01, t = 0.1, \omega = 0.5, a = 0.8$ (the second problem)

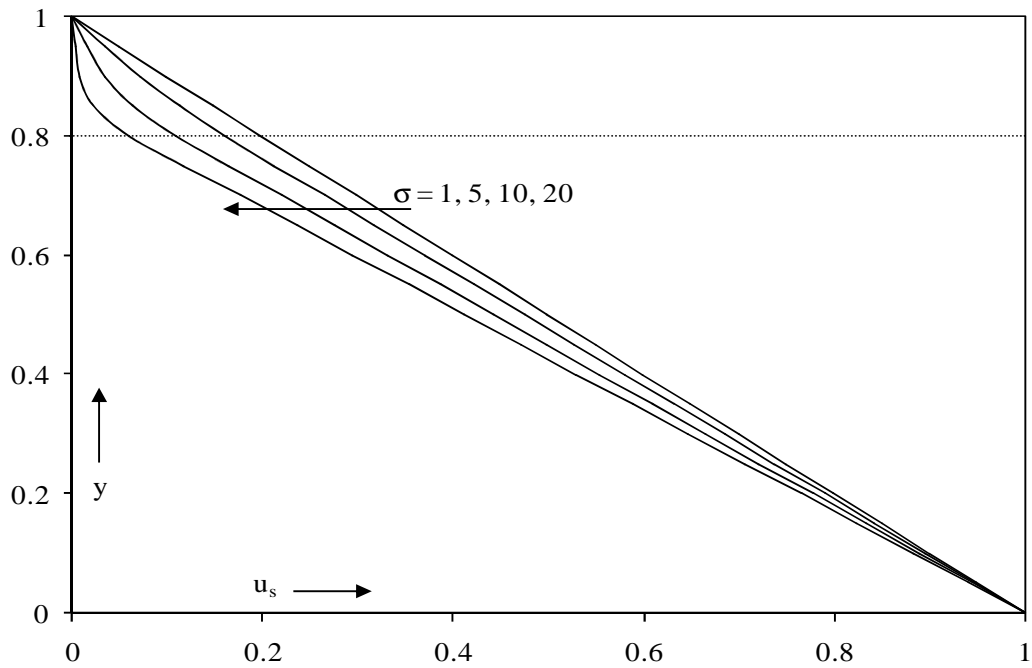


Fig. 7(a) Profiles of the dimensionless steady state velocity $u_s(y)$ against y for $\alpha = 0.01$, $t = 0.1$, $a = 0.8$ (the first problem)

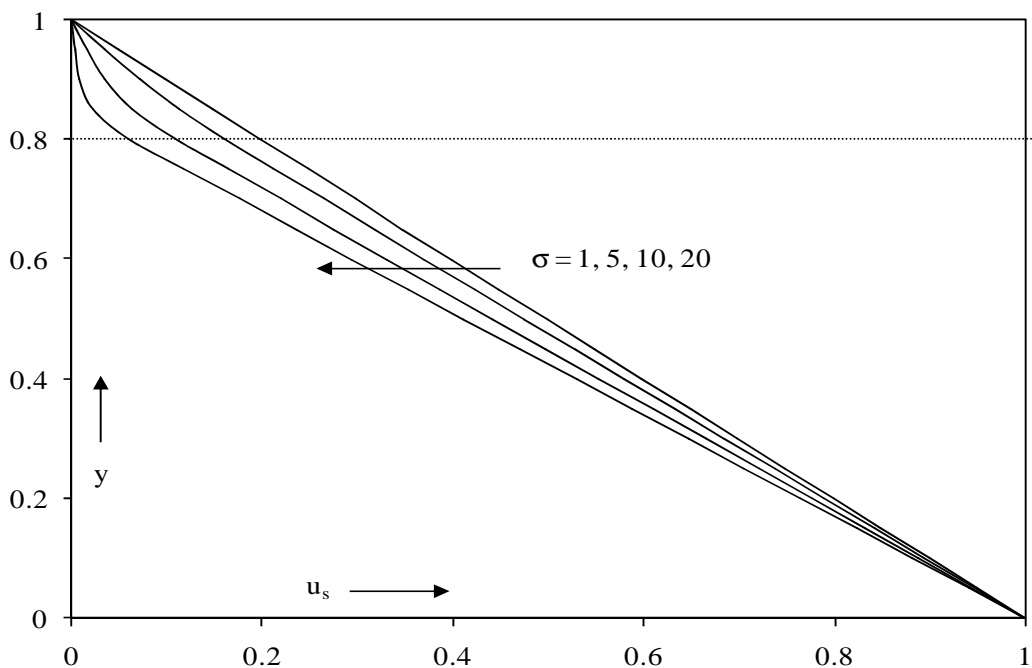


Fig. 7(b) Profiles of the dimensionless steady state velocity $u_s(y)$ against y for $\alpha = 0.01$, $t = 0.1$, $\omega = 0.5$, $a = 0.8$ (the second problem)

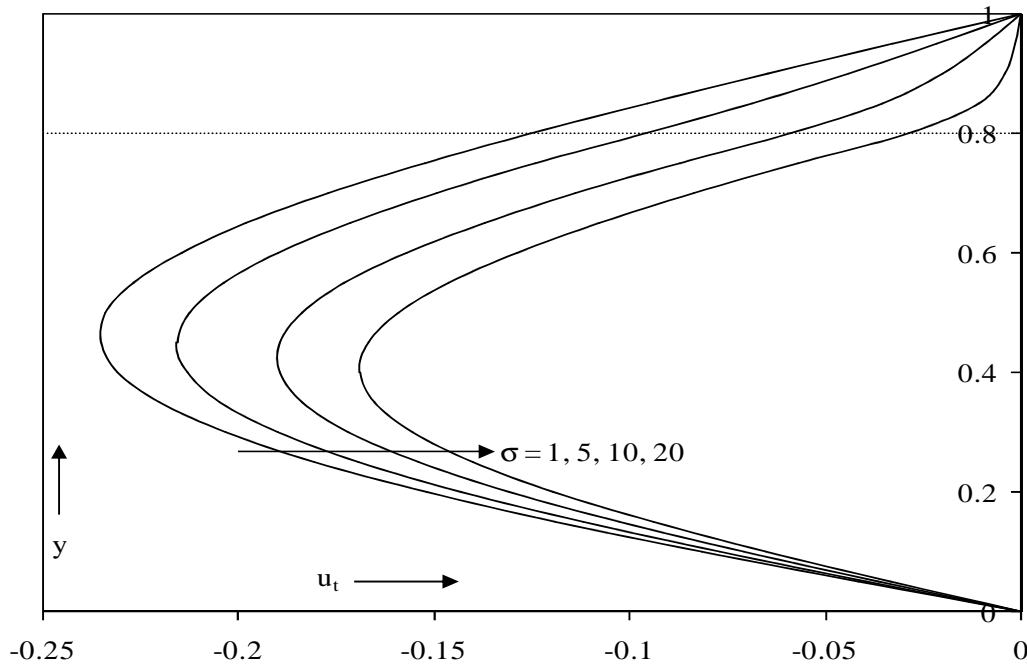


Fig. 8(a) Profiles of the dimensionless transient velocity $u_t(y)$ against y for $\alpha = 0.01$, $t = 0.1$, $a = 0.8$ (the first problem)

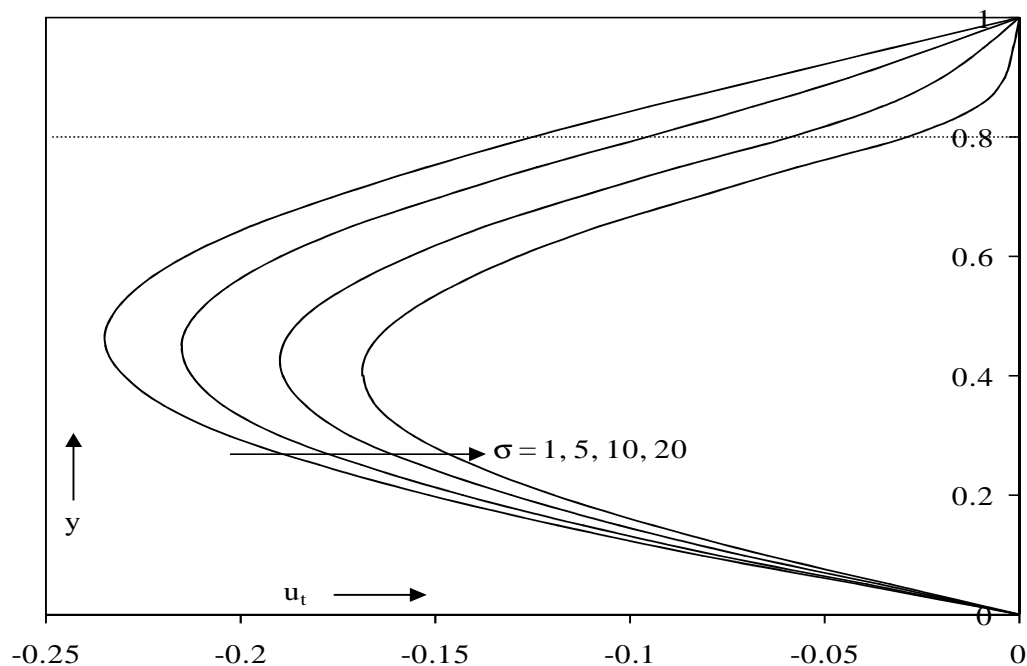


Fig. 8(b) Profiles of the dimensionless transient velocity $u_t(y)$ against y for $\alpha = 0.01$, $t = 0.1$, $\omega = 0.5$, $a = 0.8$ (the second problem)

Figures 9-11, shows variations of shear stresses at the moving/oscillating wall and at the stationary porous interface in the channel for various parameters. From the engineering application point of view, reduction in skin friction at the channel walls is important. Among several techniques for reducing skin friction, changing the wall boundary conditions such as applying suction or porous medium lining play a significant role. It is seen from fig. 9 that the

effect of the permeability of the porous layer is to reduce the dimensionless shear stress at the channel walls for both type of problems.

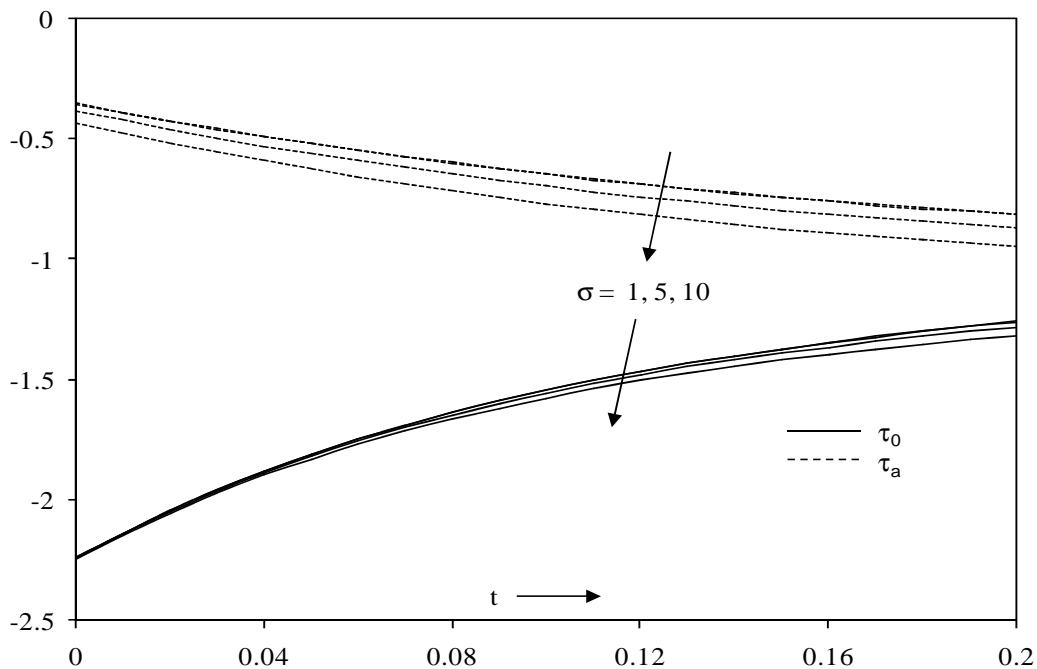


Fig. 9(a) Profiles of the dimensionless shear stress τ_{yx} against t { τ_0 - at lower plate, and τ_a - at porous medium interface} for $\alpha = 0.05, a = 0.8$ (the first problem)

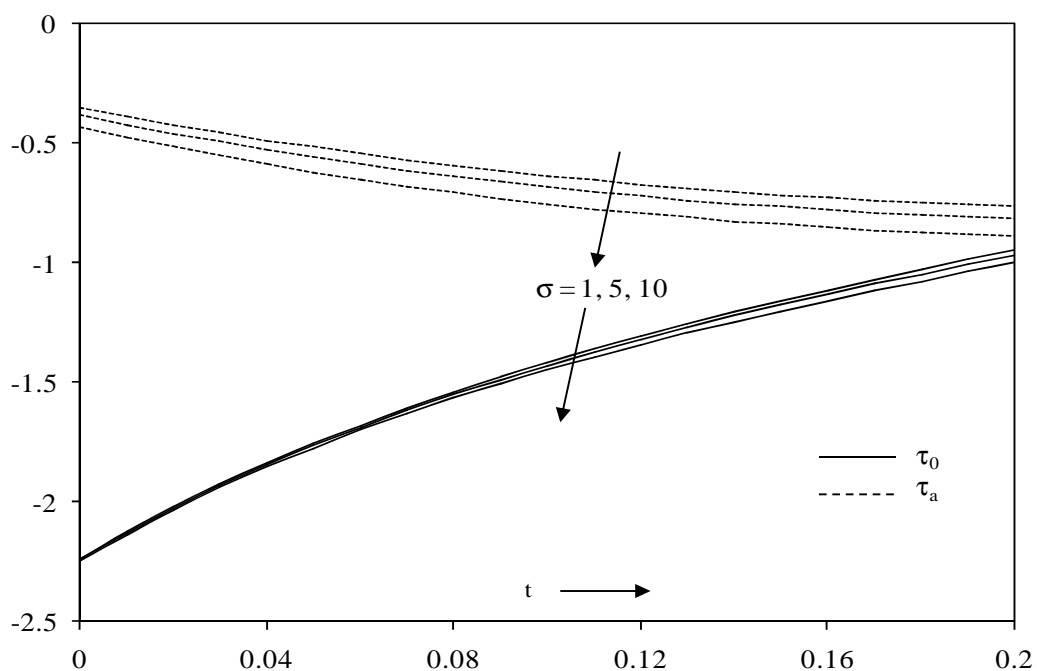


Fig. 9(b) Profiles of the dimensionless shear stress τ_{yx} against t { τ_0 - at lower plate, and τ_a - at porous medium interface} for $\alpha = 0.05, \omega = 2, a = 0.8$ (the second problem)

It is observed that as permeability K increases (or $\sigma = h \frac{\epsilon}{\sqrt{K}}$ decreases), the shear stress τ_0 at the lower wall and τ_a at the porous interface decreases absolutely. However in fig. 10 it is observe that the non-Newtonian parameter

α increases numerically the shear stress τ_a at the porous interface but decrease τ_0 at the lower wall. Figure 11 shows that the shear stress at the porous interface (τ_a) reduces numerically as frequency ω increases for small time, while the shear stress at the oscillating plate (τ_0) decreases numerically as frequency ω increases but as time passes it changes sign and increases afterwards.

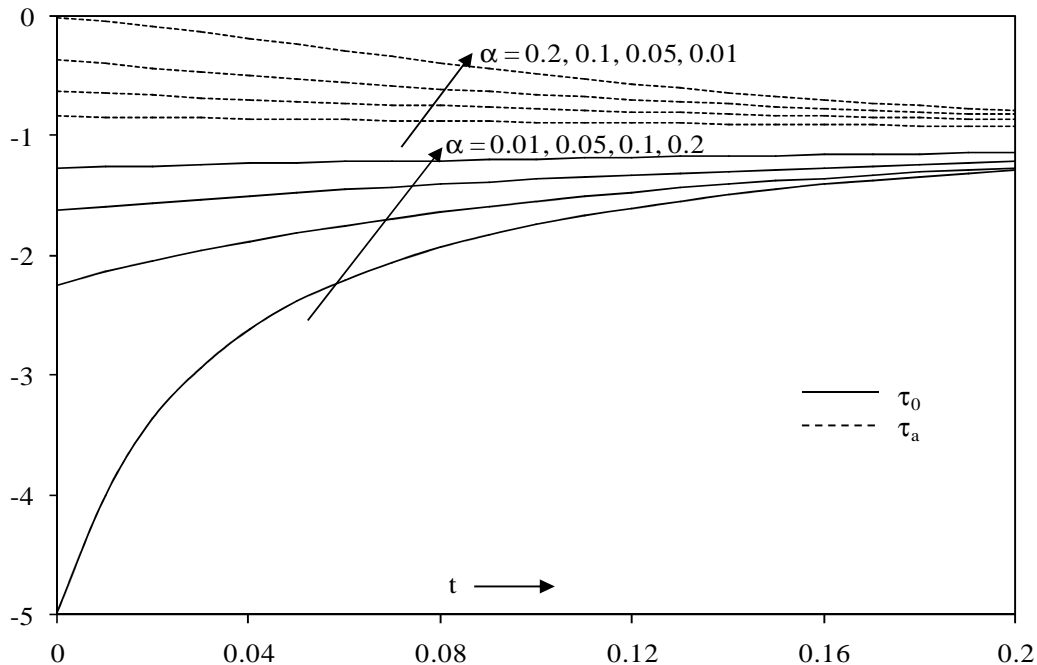


Fig. 10(a) Profiles of the dimensionless shear stress τ_{yx} against t { τ_0 - at lower plate, and τ_a - at porous medium interface} for $\sigma = 2, a = 0.8$ (the first problem)

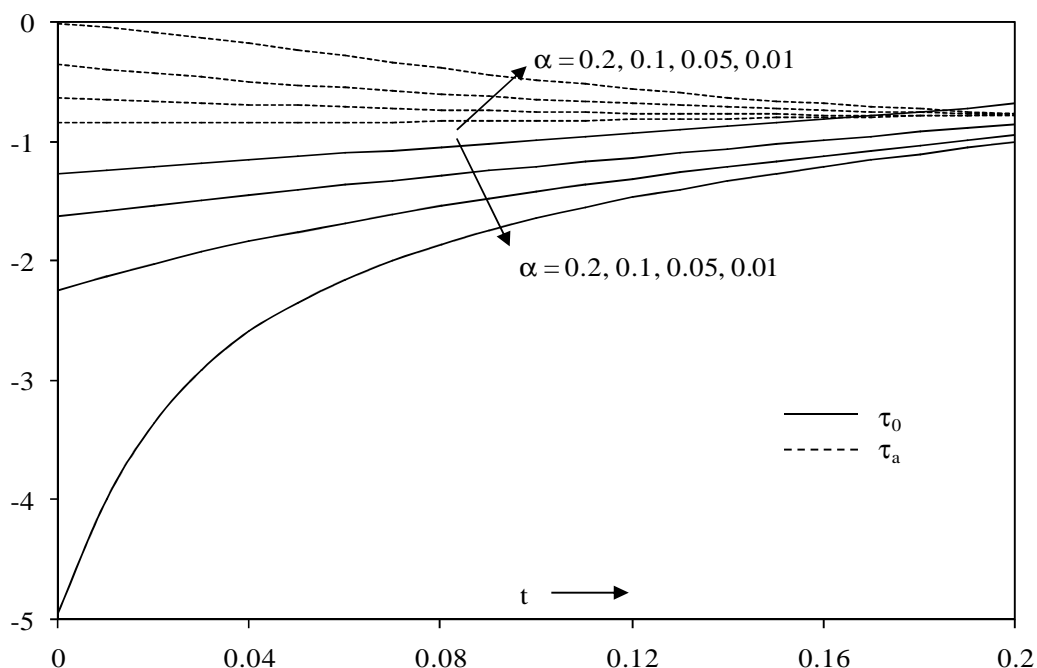


Fig. 10(b) Profiles of the dimensionless shear stress τ_{yx} against t { τ_0 - at lower plate, and τ_a - at porous medium interface} for $\sigma = 2, \omega = 2, a = 0.8$ (the second problem)

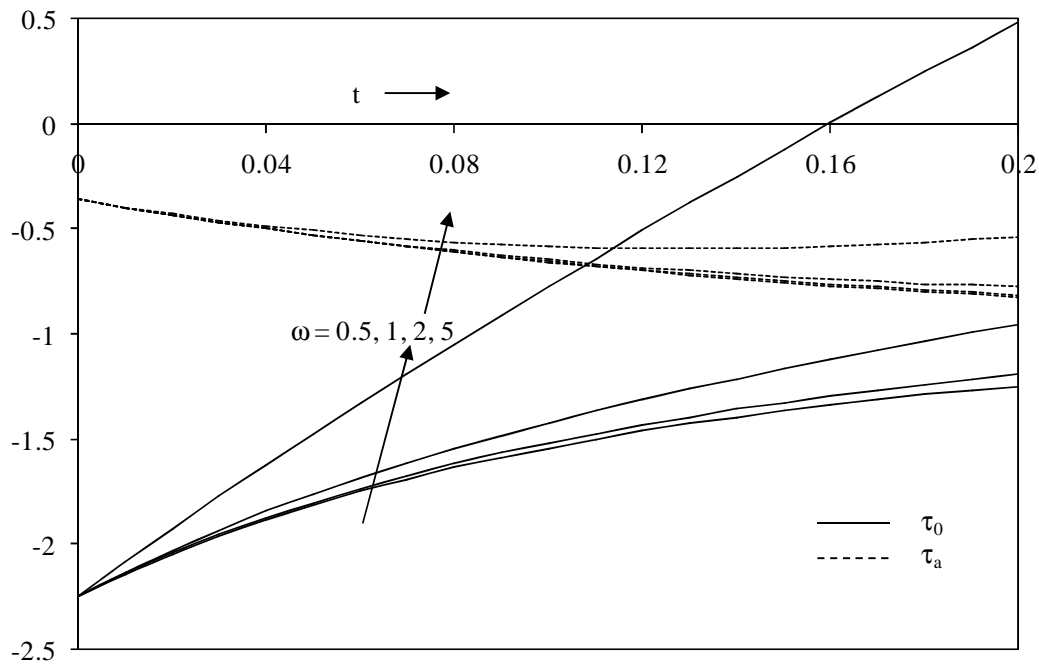


Fig. 11 Profiles of the dimensionless shear stress τ_{yx} against t (τ_0 - at lower plate, and τ_a - at porous medium interface) for $\sigma = 2$, $\alpha = 0.05$, $a = 0.8$ (the second problem)

Acknowledgements

The support provided by CSIR through Senior Research Fellowship to one of the authors Vikas Kumar is gratefully acknowledged.

REFERENCES

- [1] M. A. Al-Nimr, Khadrawi, A. F., *Transport in Porous Media*, **2003**, 51, 157-172.
- [2] O. A. Bég, H. S. Takhar, J. Zueco, A. Sajid, R. Bhargava, *Acta Mech.*, **2008**, 129-144.
- [3] D. S. Chauhan and P. Rastogi, *Appl. Math. Sci.*, **2010**, 4(13), 643-655.
- [4] D. S. Chauhan and R. Agrawal, *J. of Eng. Phy. and Thermophysics*, **2011**, 84(5), 1034-1046.
- [5] D. S. Chauhan and R. Agrawal, *Meccanica*. DOI- 10.1007/s11012-011-9446-9.
- [6] S. S. Saxena, G. K. Dubey, *Adv. in Appl. Sci. Res.*, **2011**, 2(4), 259-278.
- [7] S. Sreekanth, R. Saravana, S. Venkataramana, R. H. Reddy, *Adv. in Appl. Sci. Res.*, **2011**, 2(3), 246-264.
- [8] S. Sreenadh, S. N. Kishore, A. N. S. Srinivas, R. H. Reddy, *Adv. in Appl. Sci. Res.*, **2011**, 2(6), 215-222.
- [9] M. S. Babu, P. V. S. Narayana, T. S. Reddy, D. U. Reddy, *Adv. in Appl. Sci. Res.*, **2011**, 2(5), 226-239.
- [10] S. K. Bhargava, N. C. Sacheti, *Indian Journal of Technology*, **1989**, 27, 211-214.
- [11] J. Daskalakis, *Int. J. of Energy Research*, **1990**, 14, 21-26.
- [12] A. Nakayama, *ASME Journal of Fluids Engineering*, **1992**, 114, 642-647.
- [13] D. S. Chauhan, K. S. Shekhawat, *J. Phys. D: Appl. Phys.*, **1993**, 26, 933-936.
- [14] D. S. Chauhan, V. Soni, *AMSE Periodicals: Modeling Measurement & Control B*, **1994**, 56, 7-21.
- [15] A. V. Kuznetsov, *Int. J. Heat Mass Transfer*, **1998**, 41, 2556-2560.
- [16] D. S. Chauhan, S. Gupta, *AMSE Periodicals: Mod. Meas. & Control B*, **1999**, 67, 37-52.
- [17] A. V. Kuznetsov, *Acta Mech.*, **2000**, 140, 163-170.
- [18] K. D. Singh, *ZAMP*, **1999**, 50, 661-668.
- [190] A. Govindarajan, V. Ramamurthy, K. Sundarammal, *Journal of Zhejiang University SCIENCE A*, **2007**, 8, 313-322.
- [20] D. S. Chauhan, V. Kumar, *Appl. Math. Sci.*, **2010**, 4, 2683-2695.
- [21] P. M. Jordan, P. Puri, *Proc. Roy. Soc. Lond. A*, **2002**, 458, 1245-1272.
- [22] A. R. A. Khaled, K. Vafai, *Int. J. Non-Linear Mech.*, **2004**, 39, 795-809.
- [23] H. A. Attia, *Kragujevac J. Sci.*, **2005**, 27, 23-30.
- [24] H. A. Attia, *Comm. Nonlinear Sci. Numer. Simulation*, **2008**, 13, 1596-1604.
- [25] O. A. Bég, J. Zueco, H. S. Takhar, *Commun. Nonlinear Sci. Numer. Simulat.*, **2009**, 14, 1082-1097.
- [26] J. C. Umavathi, A. J. Chamkha, A. Mateen, A. Al-Mudhaf, *Nonlinear Analysis: Mod. and Cont.*, **2009**, 14, 397-415.

- [27] W. Tan, L. Wei, F. Xian, *Chinese Sci. Bull.*, **2002**, 47, 1783-1785.
- [28] W. Tan, M. Xu, *Acta Mech. Sinica*, **2004**, 20, 471-476.
- [29] M. E. Erdoğlan, C. E. İmrak, *Int. J. Nonlinear Mech.*, **2004**, 39, 1379-1384.
- [30] P. M. Jordan, P. Puri, *Int. J. Nonlinear Mech.*, **2003**, 38, 1019-1025.
- [31] W. Tan, T. Masuoka, *Int. J. Nonlinear Mech.*, **2005**, 40, 515-522.
- [32] T. Hayat, M. Khan, M. Ayub, A. M. Siddiqui, *Arch. Mech.*, **2005**, 57, 405-416.
- [33] R. L. Fosdick, K. R. Rajagopal, *Int. J. Nonlinear Mech.*, **1978**, 13, 131-137.
- [34] J. E. Dunn, K. R. Rajagopal, *Int. J. Eng. Sci.*, **1995**, 33, 689-729.
- [35] K. Vafai, C. L. Tien, *Int. J. Heat Mass Transfer*, **1981**, 24, 195-203.
- [36] J. W. Brown, R. V. Churchill, *Complex Variables and Applications*, 6th ed., McGraw-Hill, New York, **1995**.